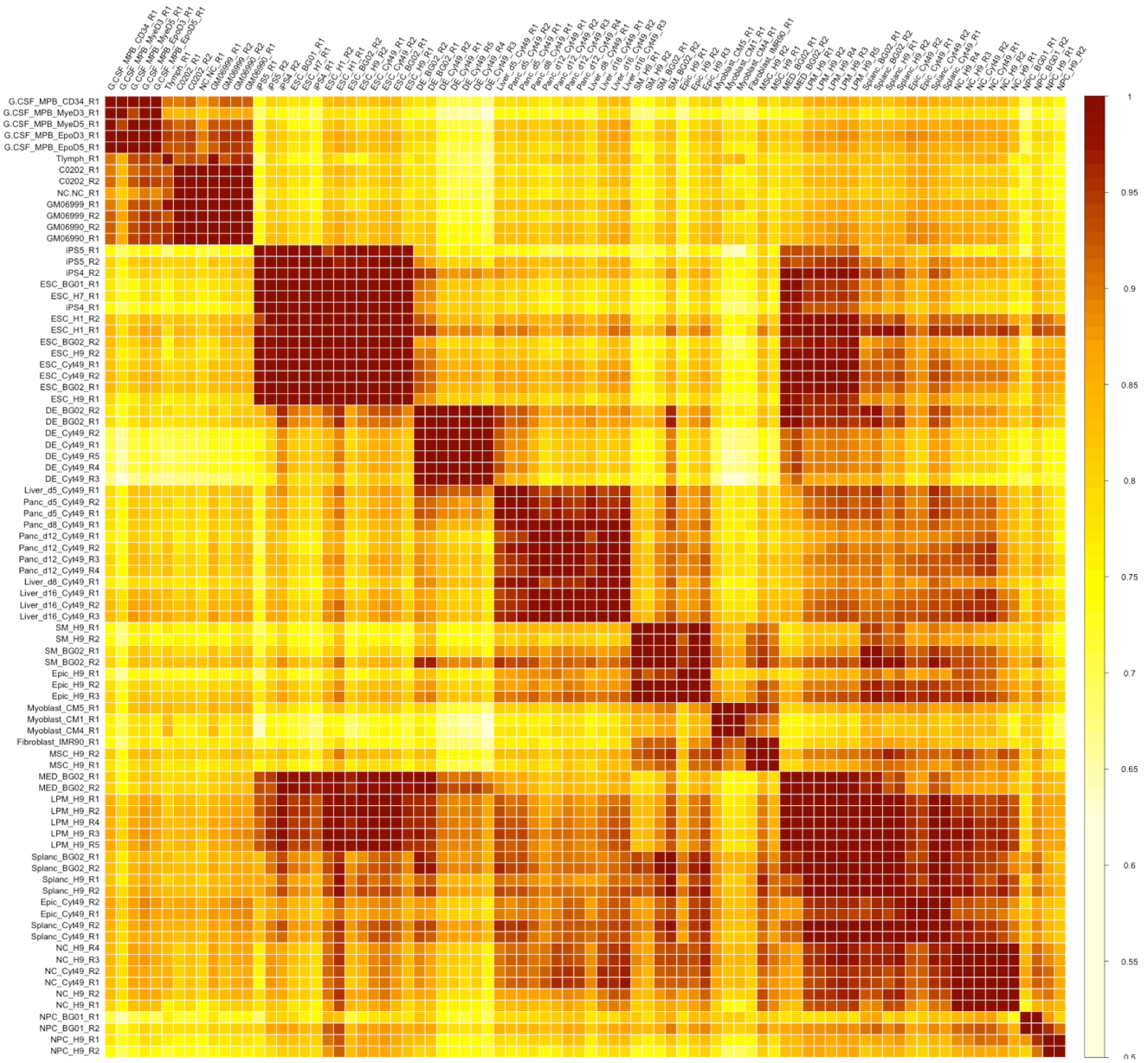


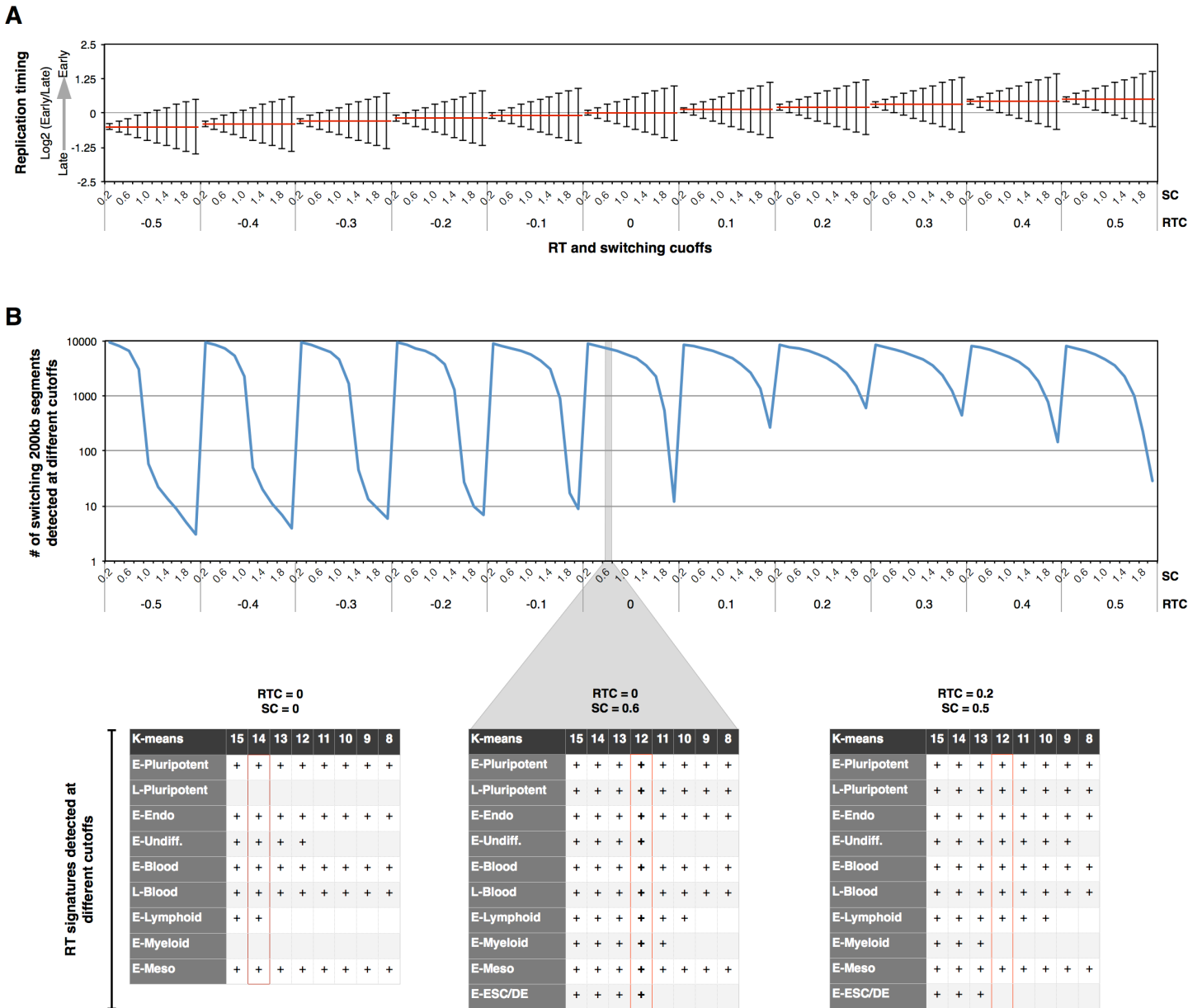
Supplementary figure 1



Supplementary Figure 1

Biological replicates have the strongest correlation values. A correlation matrix of all the samples profiled ($n=84$) using the whole genome divided in 13,305 windows of 200kb is shown, as opposed to Figure 1, which selects the RT-switching segments. The sex chromosomes were discarded from the analysis to discard gender differences. The color bar represents the correlation values.

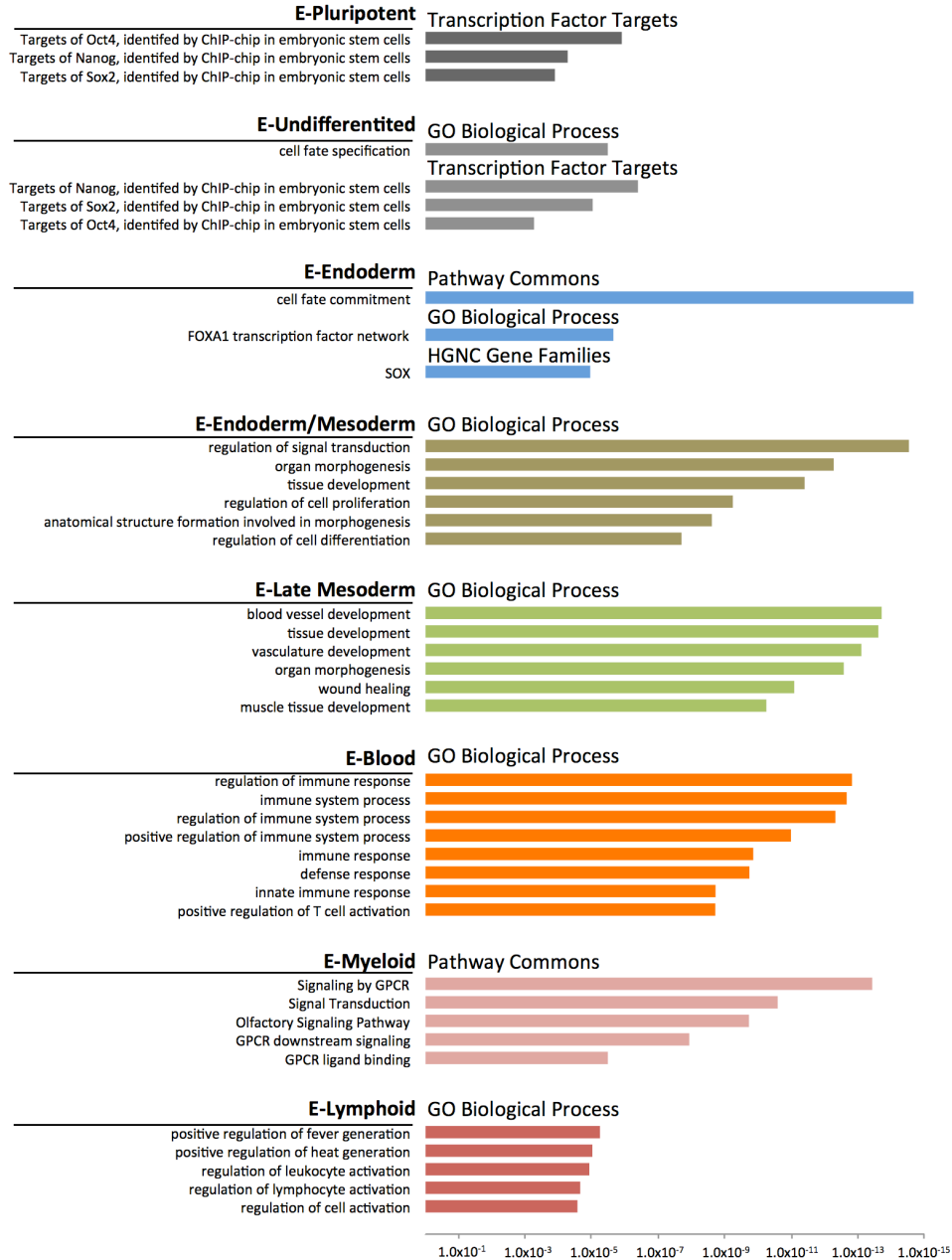
Supplementary figure 2



Supplementary Figure 2

RT and switching cutoffs used to identify the RT-switching regions (200 kb segments). (A) Graphical depiction of the RT and switching cutoffs. The “RT cutoff” (RTC) defines the point of log2 ratio at which the changes are determined, “switching cutoff” (SC) refers to the size of the change and is depicted as the maximum and minimum vertical lines. (B) Frequency of RT-switching 200kb segments using distinct RT and switching cutoffs and the RT signatures identified using distinct exemplary combinations of cutoffs. Distinct combinations of cutoffs were tested to select the parameters that best distinguished cell types (RT signature identification).

Supplementary figure 3

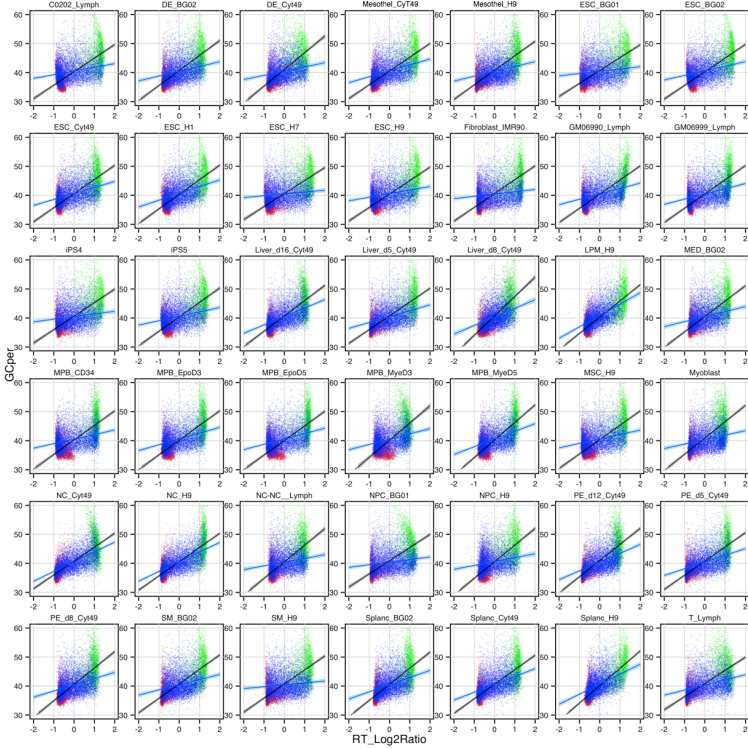


Supplementary Figure 3

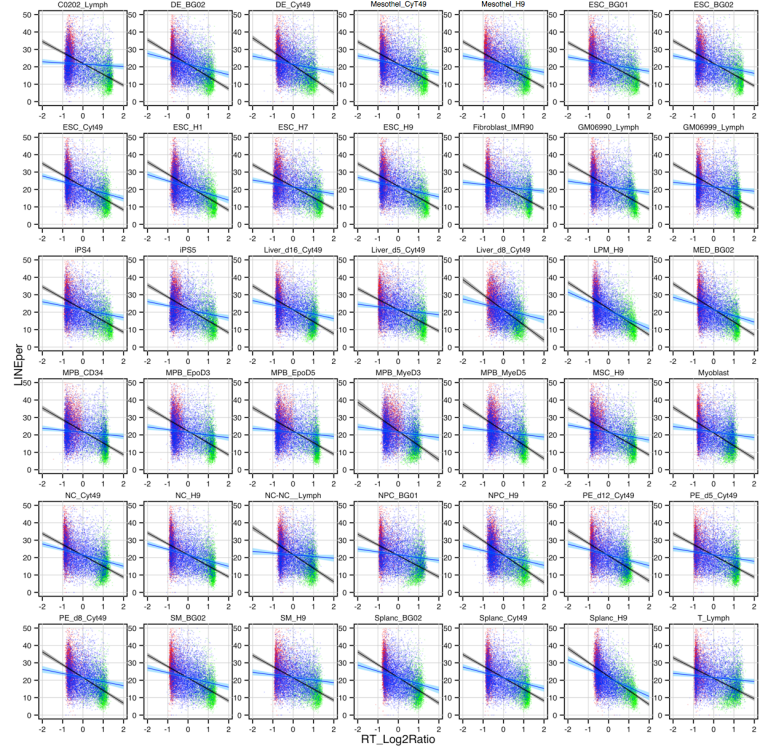
Ontology analysis of the distinct RT signatures. Analysis was performed with the Genomic Regions Enrichment of Annotations Tool (GREAT)(McLean et al. 2010) using the distinct RT signatures of 200 kb segments obtained by K-means clustering (Figure 1D). At the bottom is shown the statistical significance (p -values measured by binomial test).

Supplementary figure 4

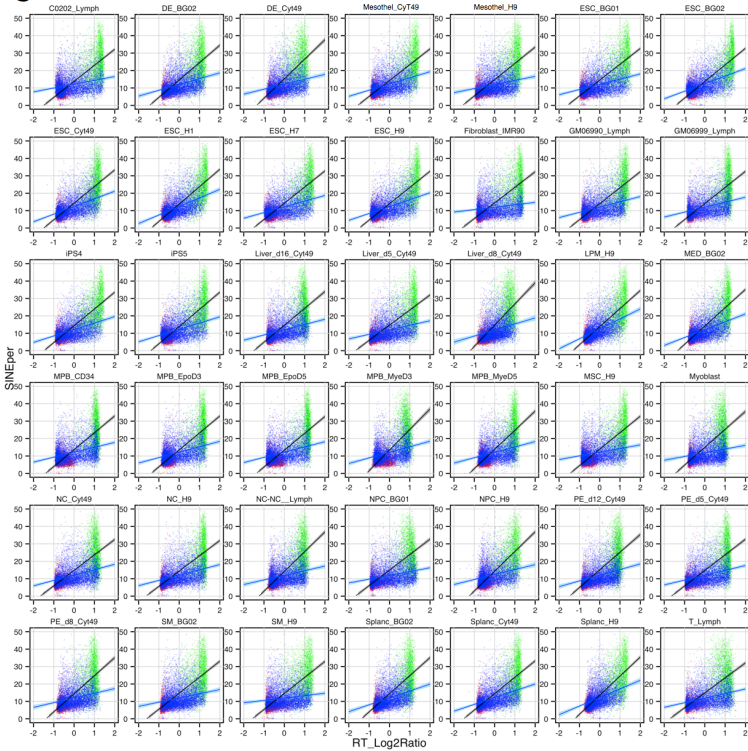
A



B



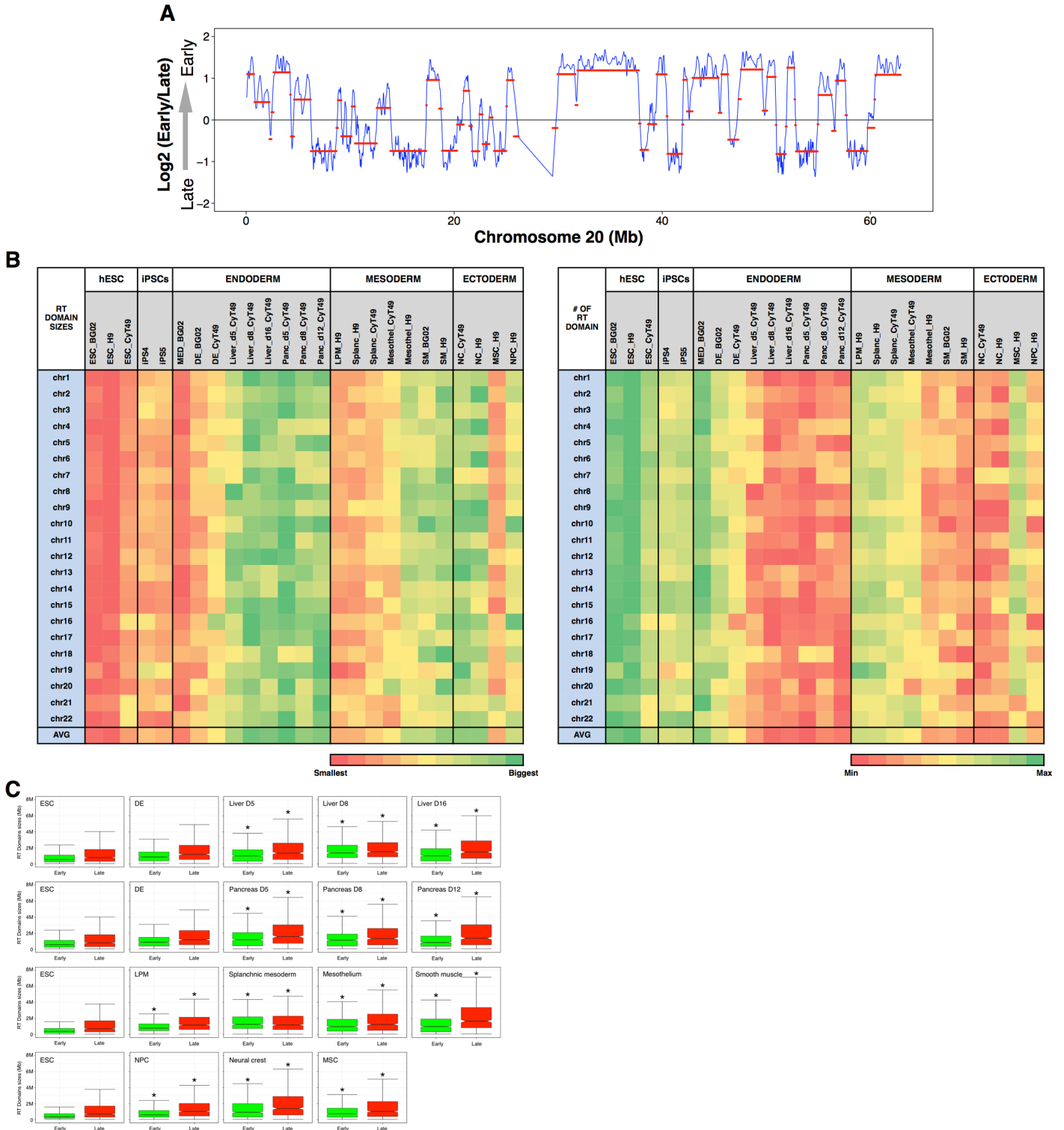
C



Supplementary Figure 4

Scatterplots and correlation of RT with GC (A) content and LINEs (B) and SINEs (C) densities per cell type.

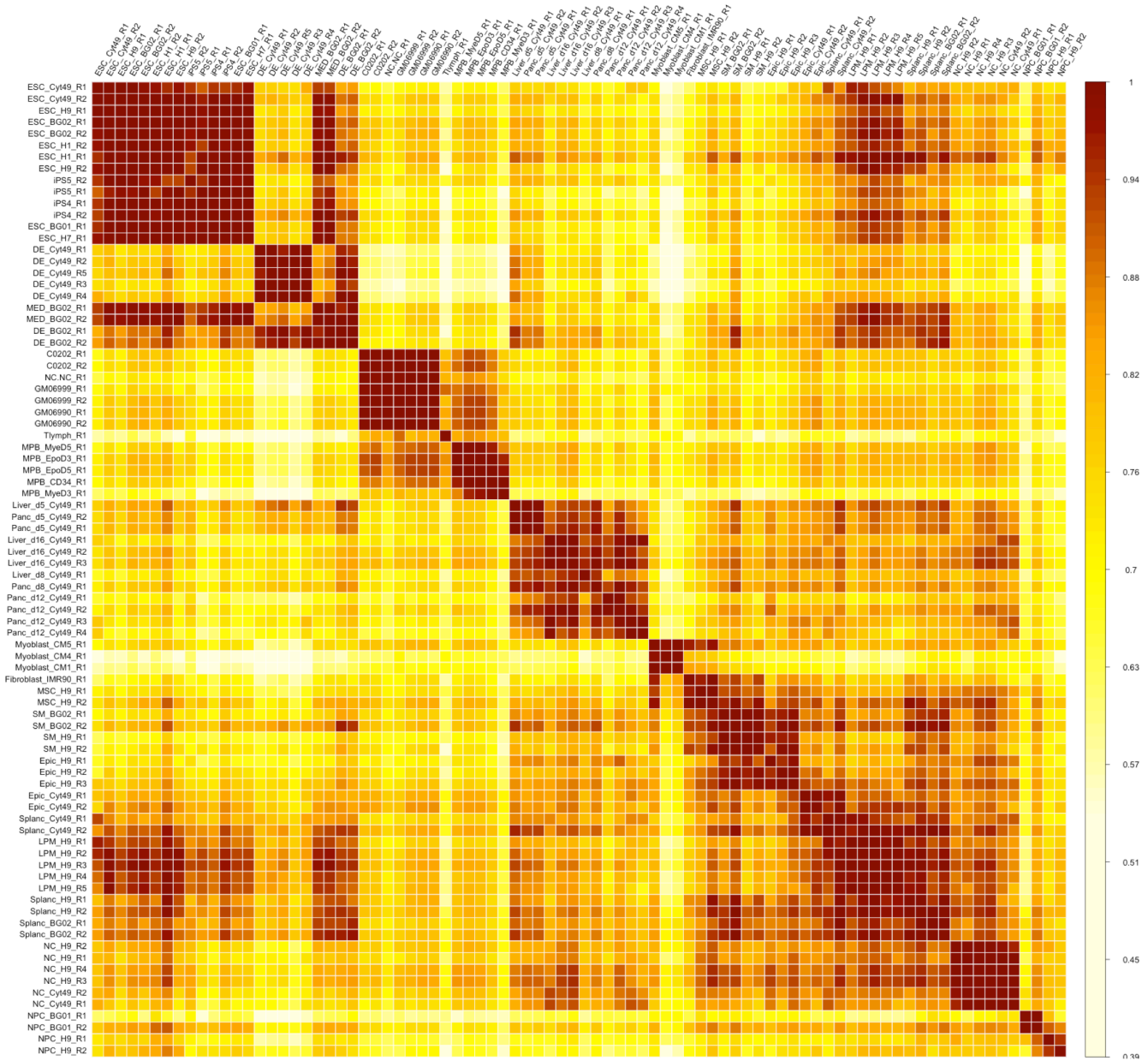
Supplementary figure 5



Supplementary Figure 5

Consolidation of replication domains during hESC differentiation. A) RT domains (RDs) of an exemplary genomic region identified by DNACopy segmentation algorithm. B) Analysis of size (left) and number (right) of RDs in all cell types per chromosome. C) Consolidation of early and late domains during differentiation towards endoderm, mesoderm and ectoderm cell types.

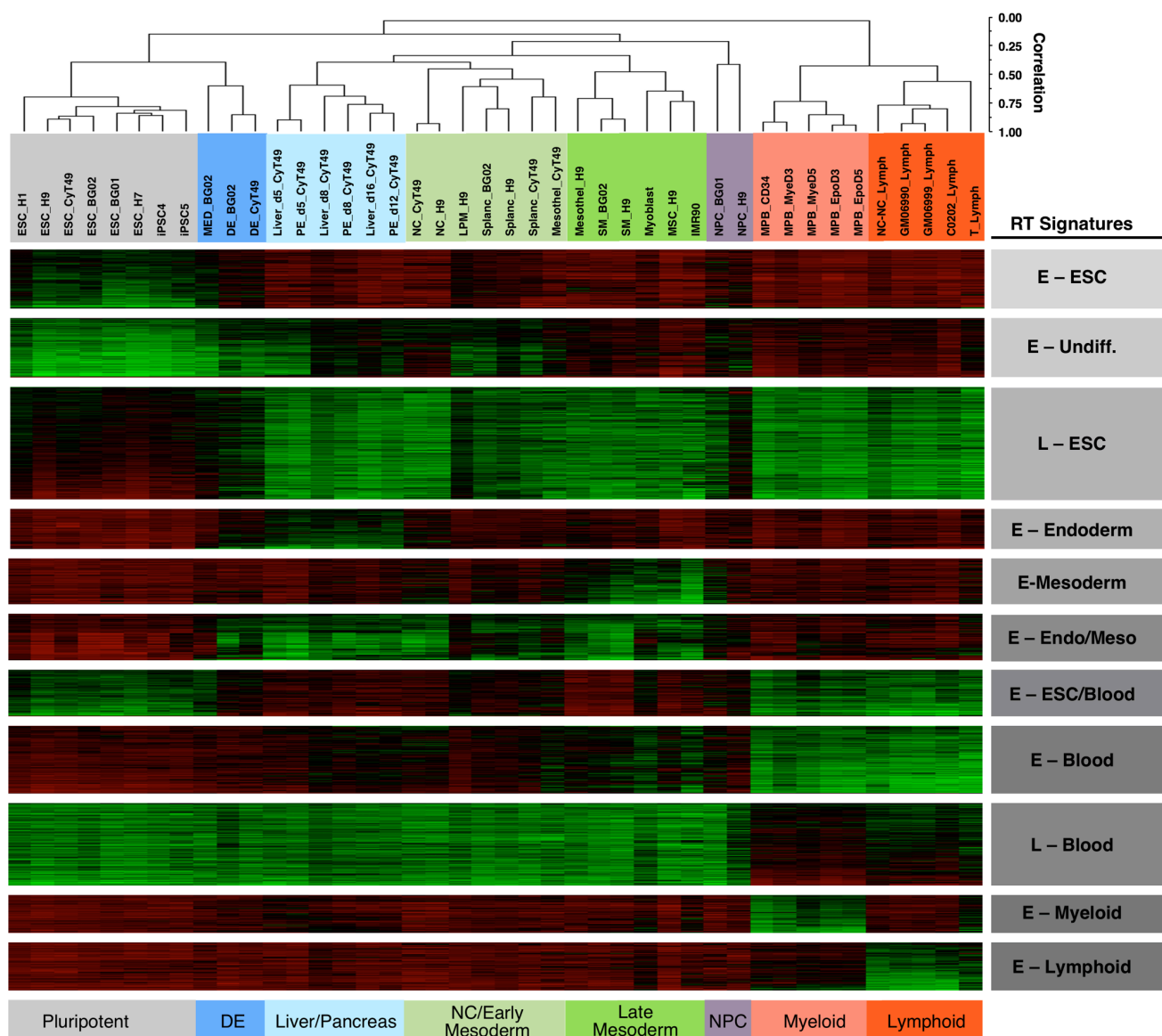
Supplementary figure 6



Supplementary Figure 6

Correlation matrix of all the samples profiled using the RT values at the TSS from 27,544 RefSeqs genes. The sex chromosomes were discarded from the analysis to discard gender differences. The color bar represents the correlation values.

Supplementary figure 7

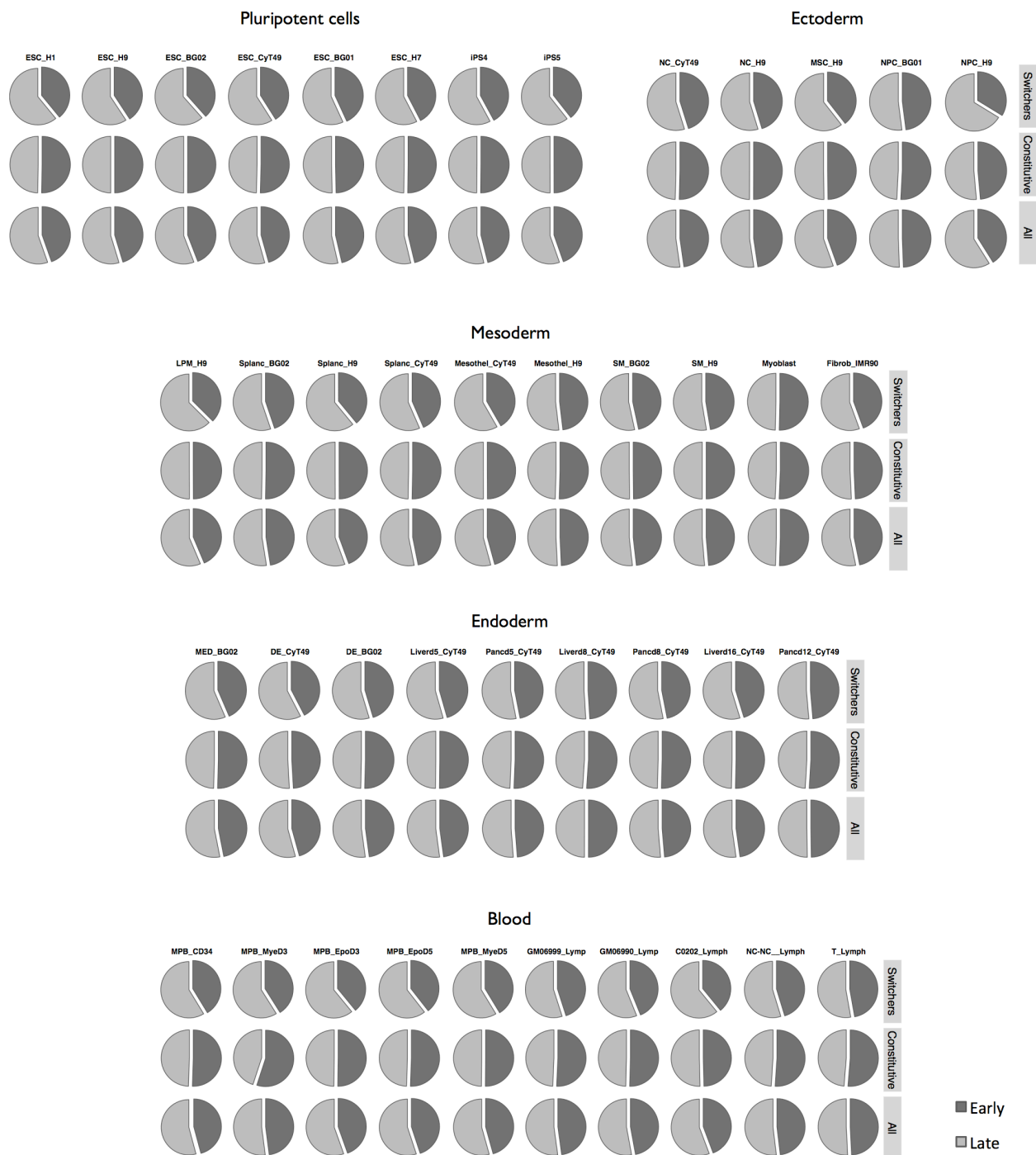


Supplementary Figure 7

Hierarchical clustering of the distinct human cell types and *k-means* clustering of RT-switching genes. RT-switching genes (27,544 RefSeqs) were used for hierarchical clustering analysis of the cell types and branches of the dendrogram were constructed based on the correlation values between distinct cell types (distance = correlation value -1). A correlation threshold of >0.6 was used to color label the major groups of cell types, specific cluster of cell types are indicated at the bottom: pluripotent, definitive endoderm, liver and pancreas, neural crest and early mesoderm, late mesoderm and fibroblasts, NPC, myeloid and lymphoid. *k-means* clustering of switching segments defined the RT signatures labeled in gray boxes.

Supplementary figure 8

200 Kb windows

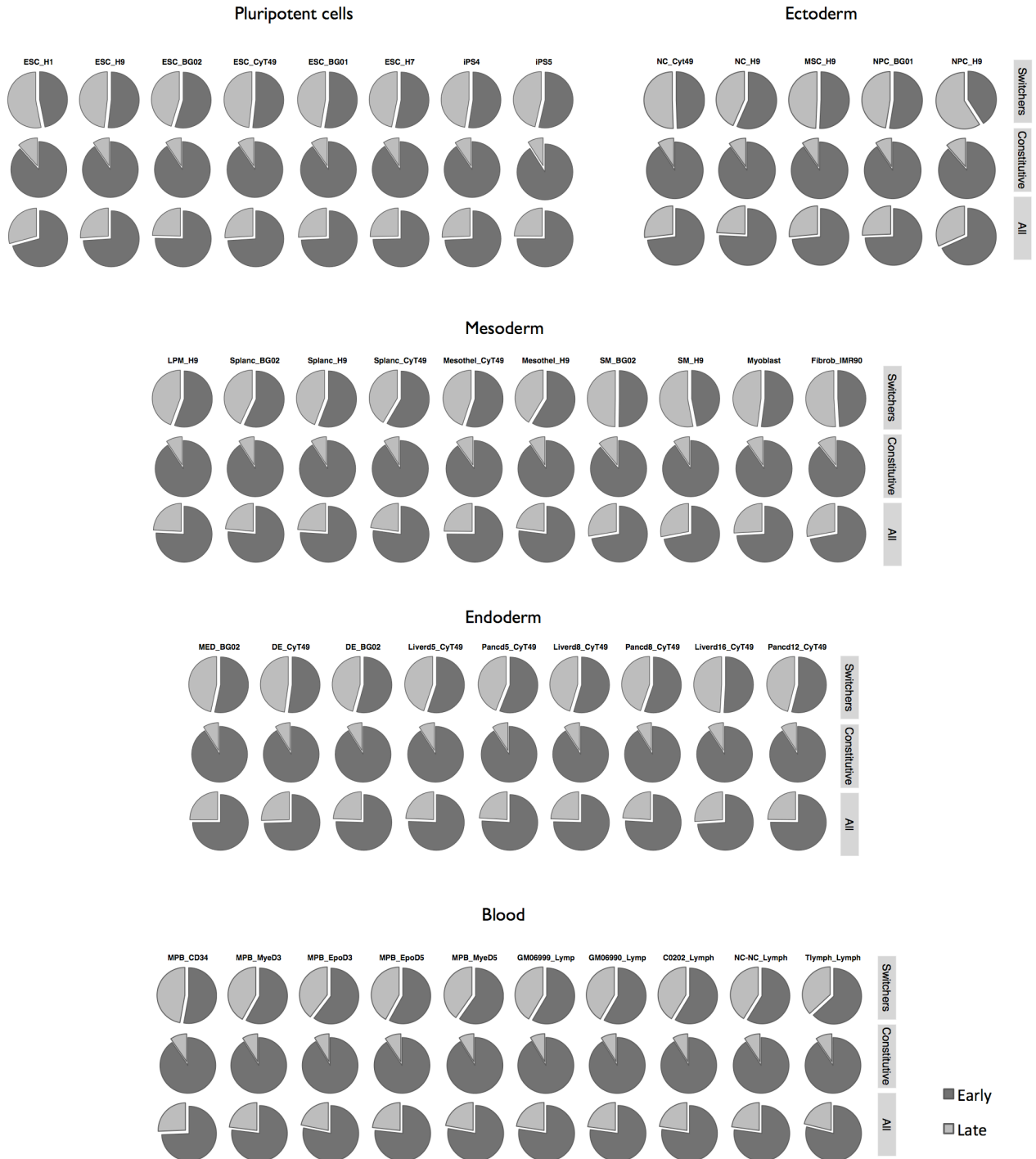


Supplementary Figure 8

Relative frequency distributions of RT-switching, RT-constitutive and all 200 kb segments in early and late S-phase fractions per cell type.

Supplementary figure 9

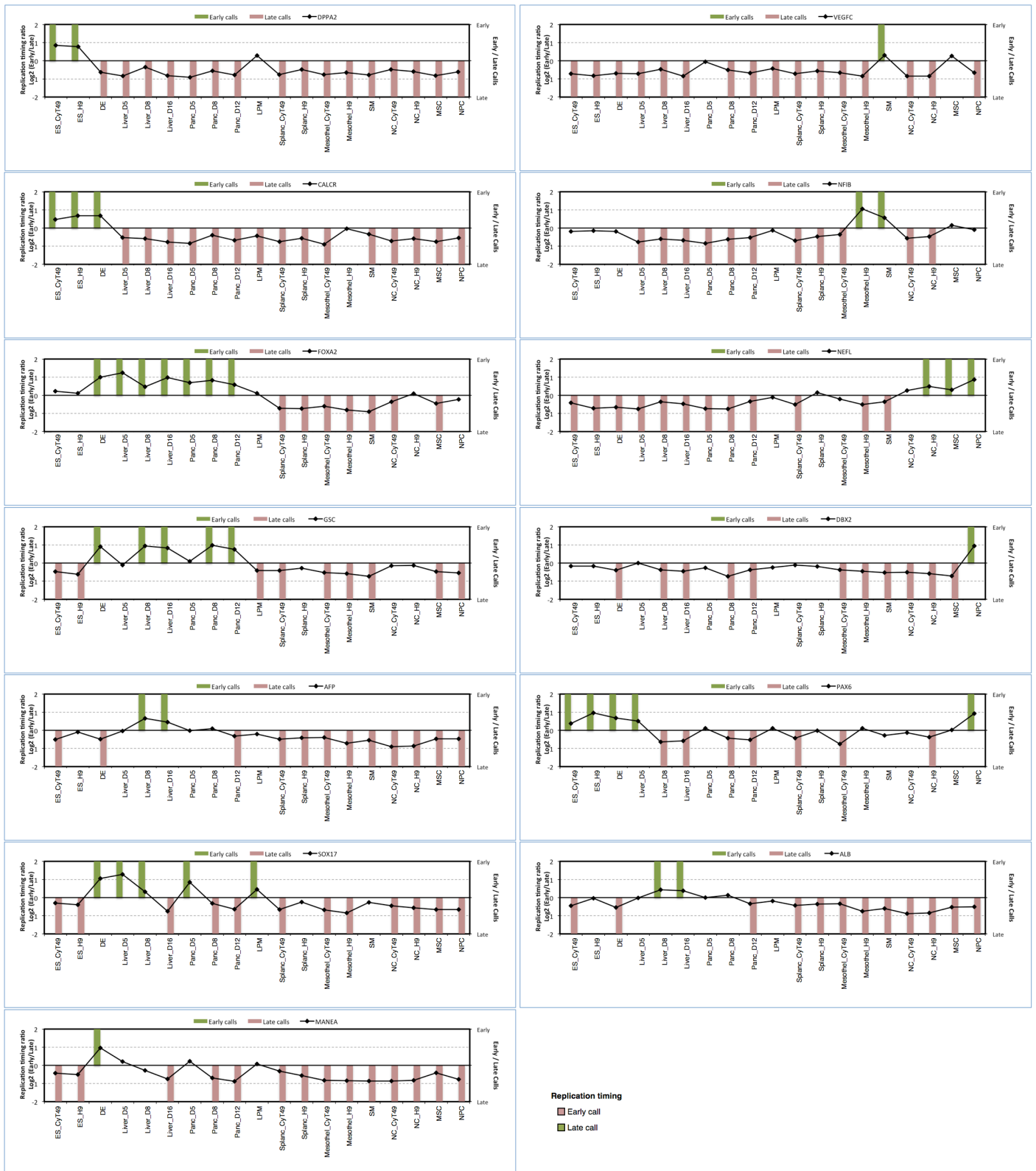
RefSeq genes



Supplementary Figure 9

Relative frequency distributions of RT-switching, RT-constitutive and all RefSeqs in early and late S-phase fractions per cell type.

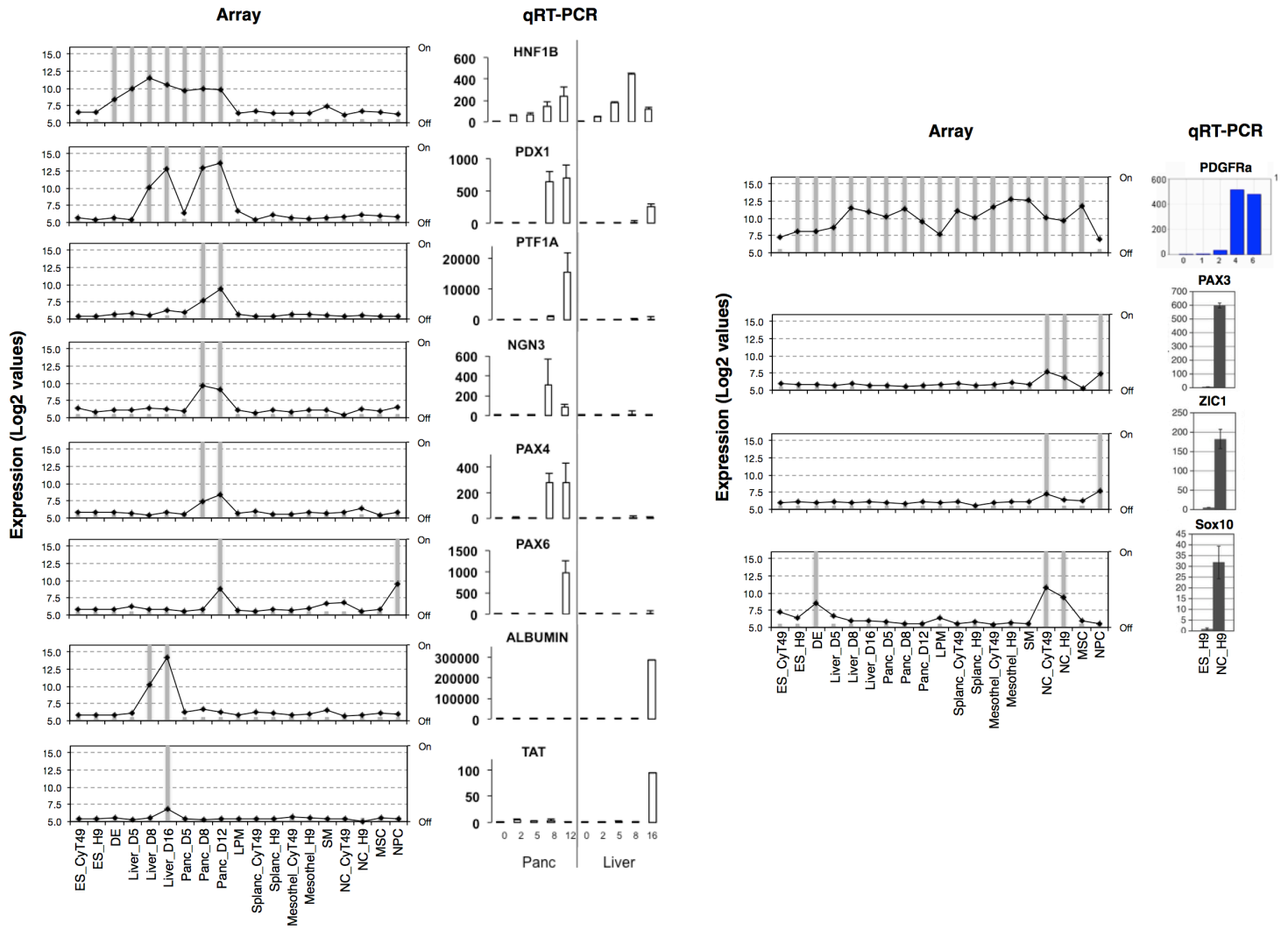
Supplementary figure 10



Supplementary Figure 10

RT of gene markers from distinct cell types. Lines represent the RT values of the specific genes across the cell types profiled. Genes were considered as early replicating if its RT log₂ ratio was $\geq +0.3$ (Early calls) and late replicating if the RT log₂ ratio was ≤ -0.3 (Late calls).

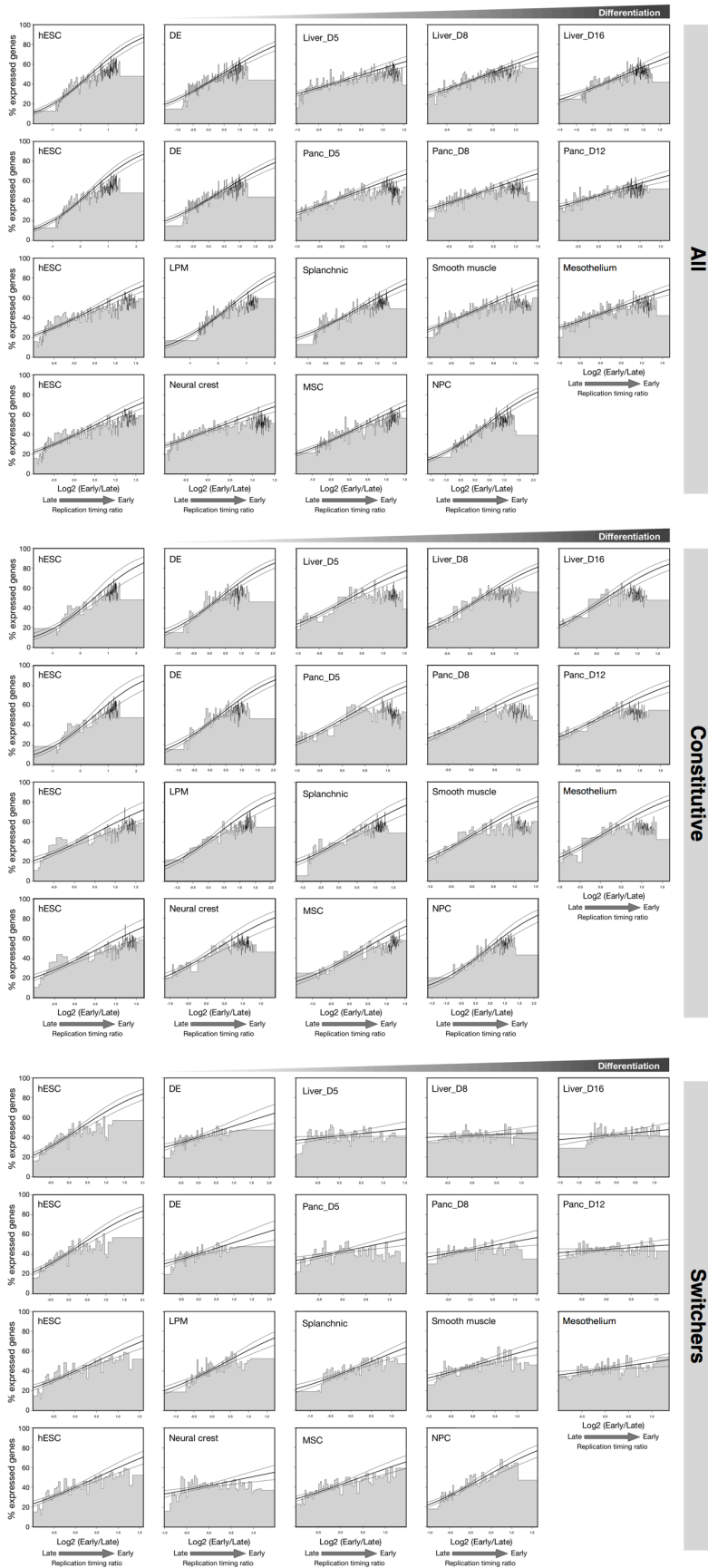
Supplementary figure 11



Supplementary Figure 11

Confirmation of gene expression by qRT-PCR using distinct specific markers for the differentiated cell types.

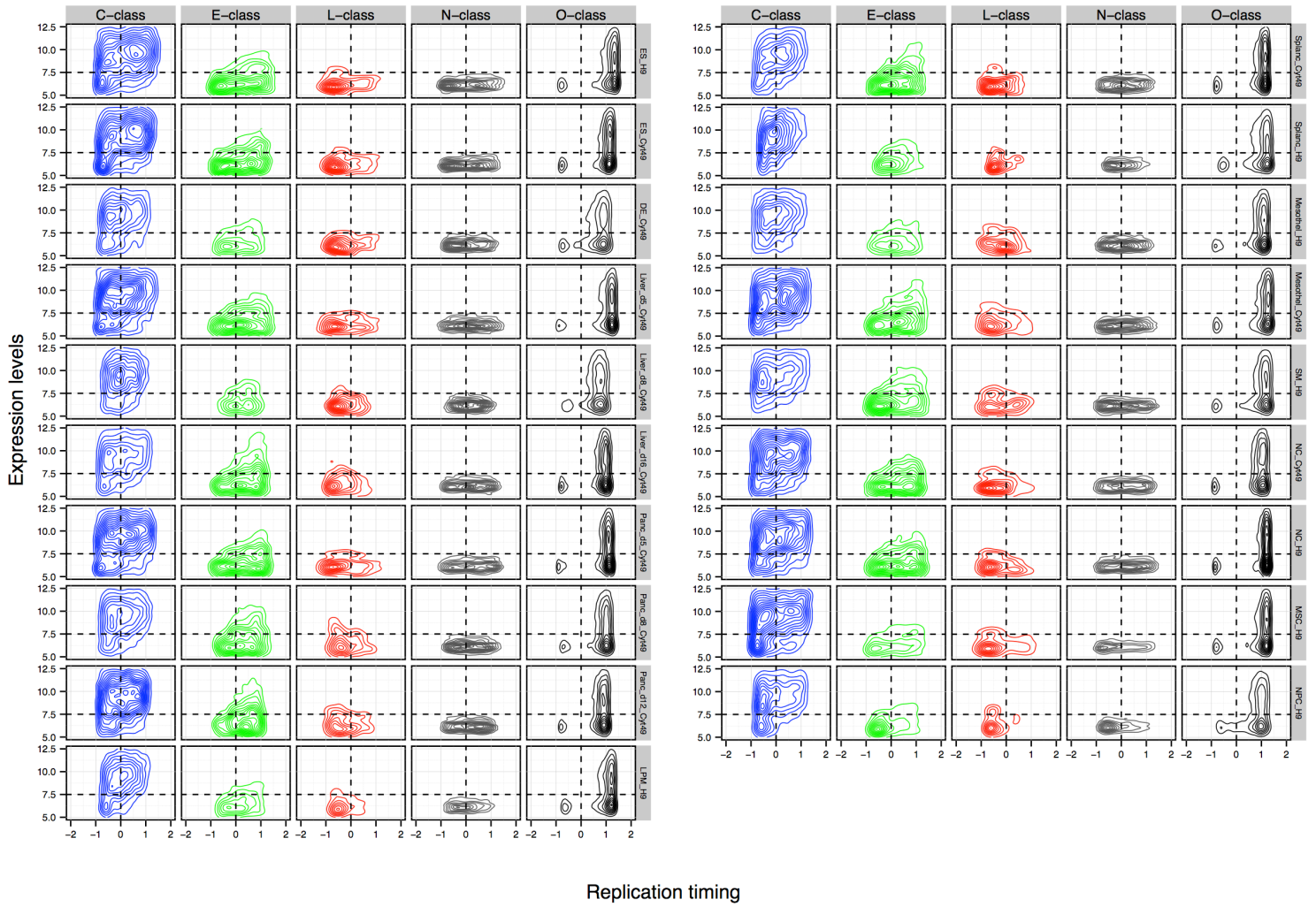
Supplementary figure 12



Supplementary Figure 12

Correlation between early replication and the probability of expression changes during differentiation in the distinct pathways comparing RT-constitutive and RT-switching genes. Genes were ranked by their RT ratio and divided into bins of 100 genes, the height of which represents the percentage of expressed genes within each bin. Logistic regression (inner line) and 95% confidence intervals (outer lines) reveal the correlation strength.

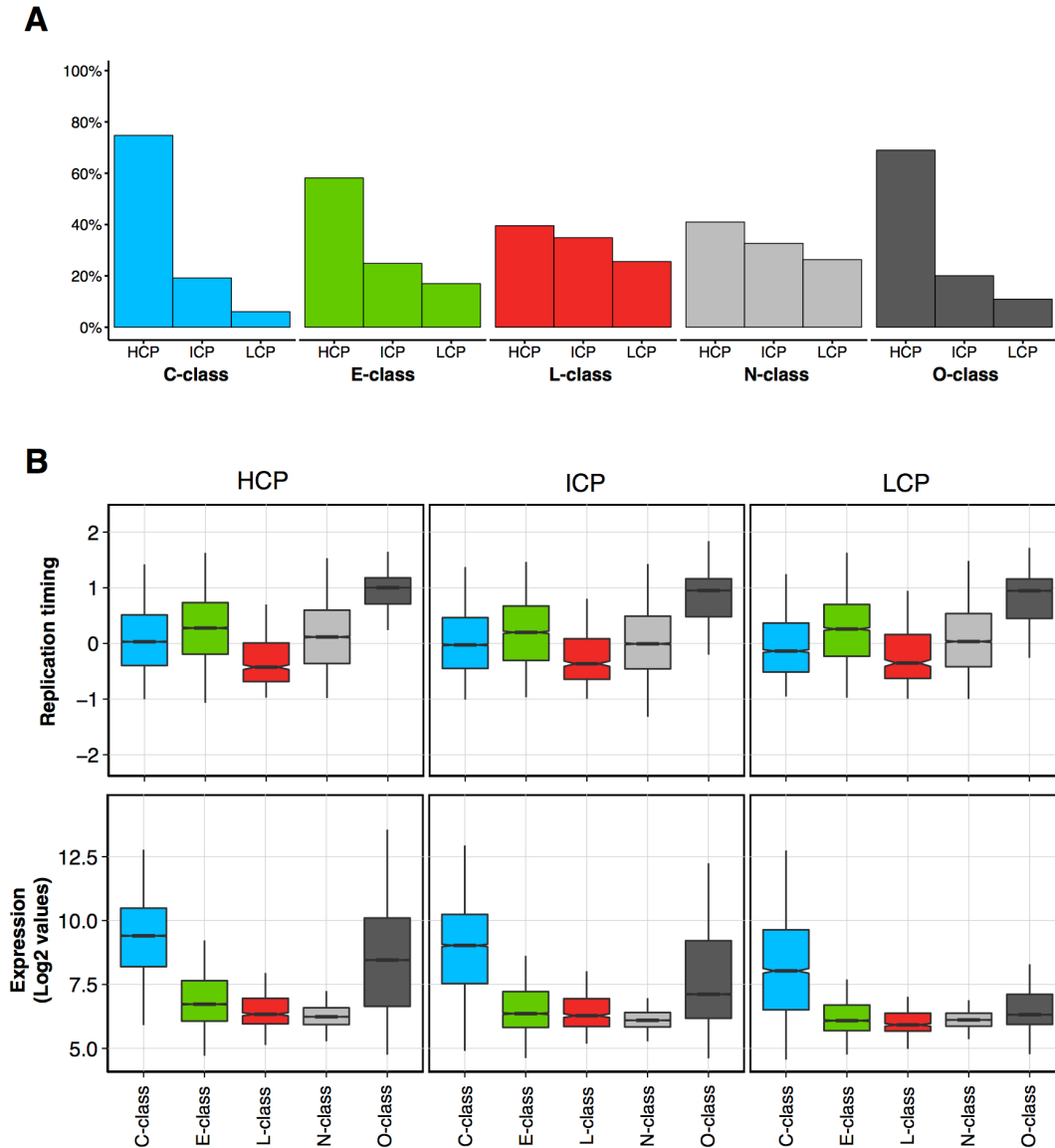
Supplementary figure 13



Supplementary Figure 13

Density plots of the distinct categories of switching genes according to their RT and transcriptional level per cell type.

Supplementary figure 14



Supplementary Figure 14

A) Frequency distributions of the distinct classes of RT-switching genes (C, E, L, O-class) among the three categories of promoters based on the CpG content at their promoters. High-CpG promoters (HCPs), intermediate-CpG (ICP) and low-CpG promoters (LCPs). B) Average RT (top graph) and transcriptional level (bottom graph) of the distinct classes of RT-switching genes (C, E, L, O-class) HCP, ICP and LCP genes.

Supplementary figure 15

ENDODERM					
RT change	C-class	E-class	L-class	N-class	O-class
EtoL	494	100	14	226	0
LtoE	361	224	11	382	0
EtoLtoE	334	155	2	185	0
LtoEtoL	307	86	17	160	0
No change in RT	943	465	42	611	10934

MESODERM					
RT change	C-class	E-class	L-class	N-class	O-class
EtoL	825	289	20	454	0
LtoE	650	312	31	441	0
EtoLtoE	0	0	0	0	0
LtoEtoL	0	0	0	0	0
No change in RT	964	429	35	669	10934

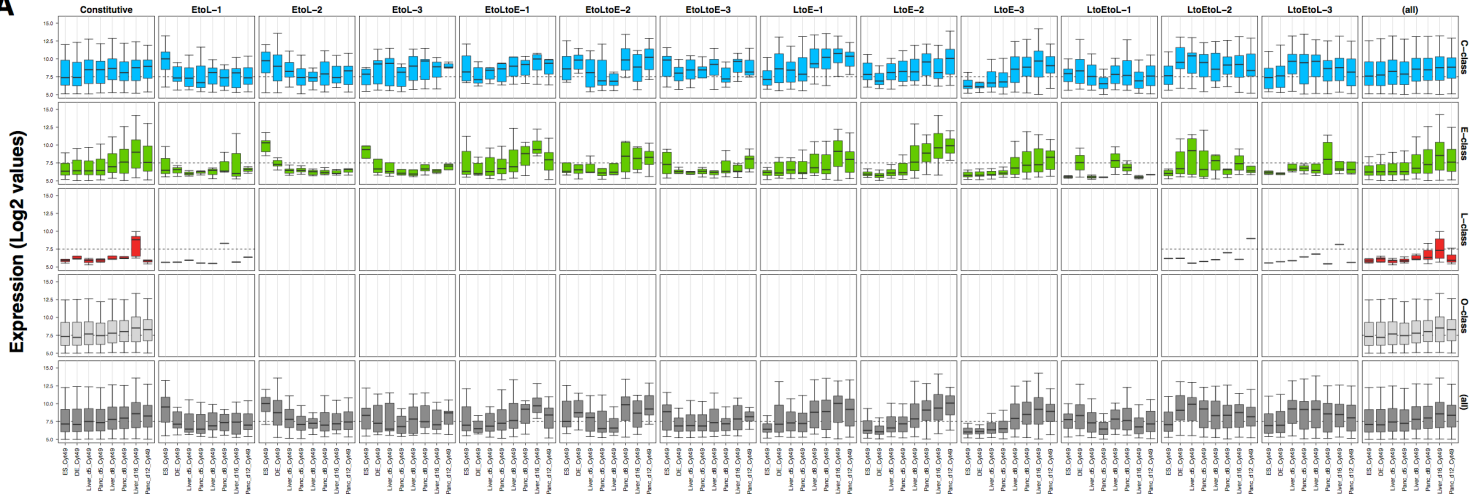
ECTODERM					
RT change	C-class	E-class	L-class	N-class	O-class
EtoL	835	357	16	539	0
LtoE	492	228	22	337	0
EtoLtoE	133	49	3	49	0
LtoEtoL	105	44	10	105	0
No change in RT	874	352	35	534	10934

Supplementary Figure 15

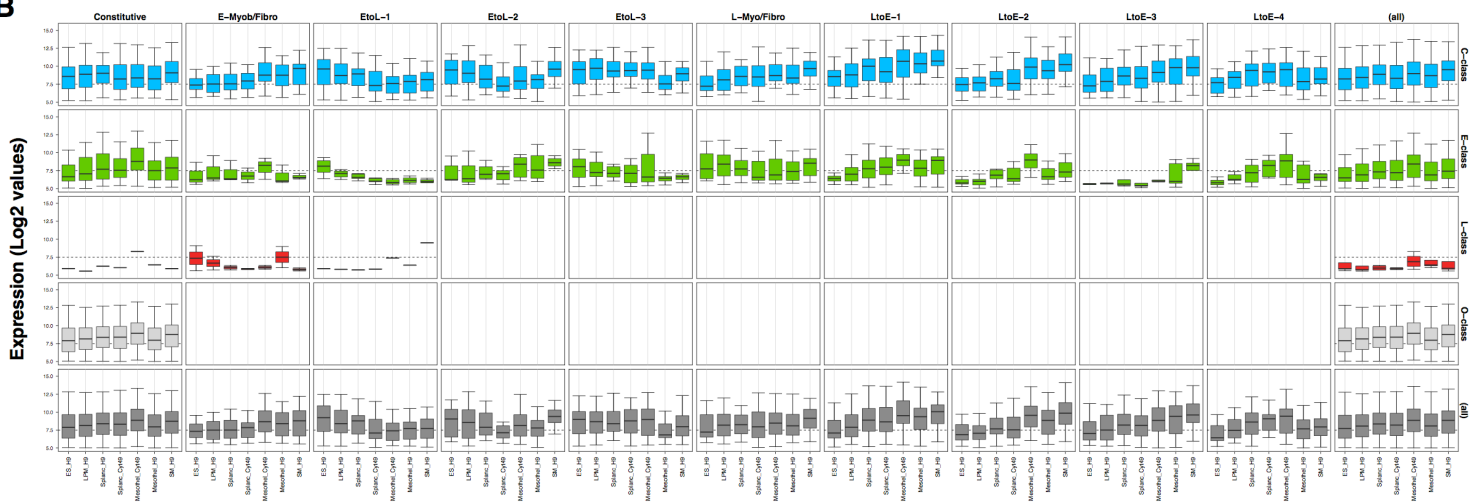
Summary of number of RT-switching genes per categories (C, E, L, N and O-class) in each RT regulation patterns (EtoL, LtoE, EtoLtoE, LtoEtoL) per differentiation pathway.

Supplementary figure 16

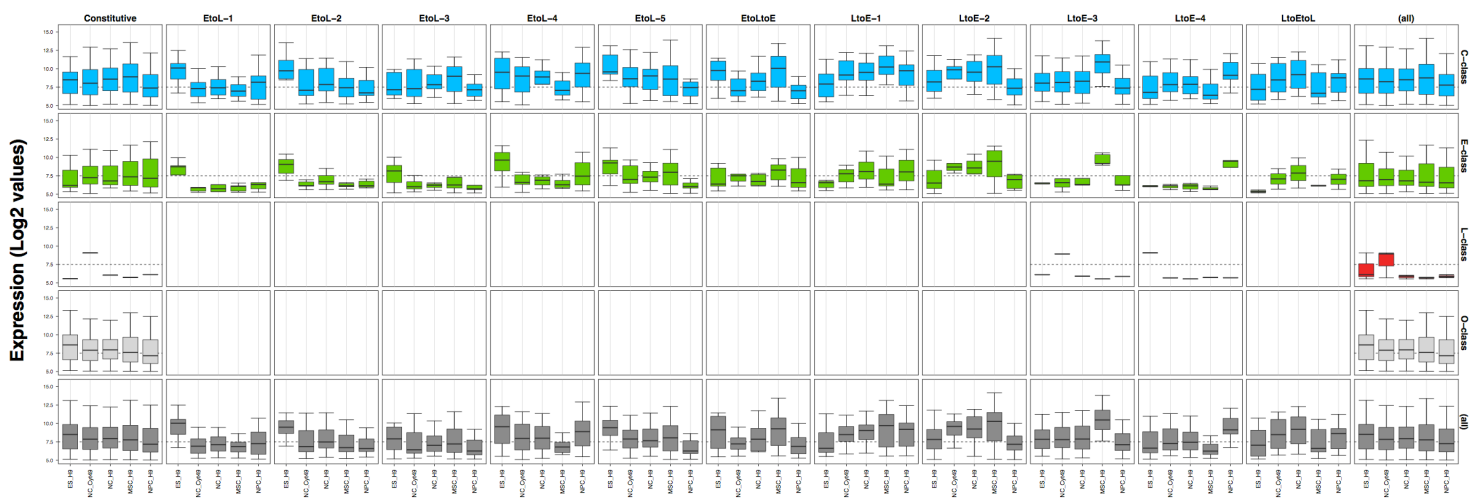
A



B



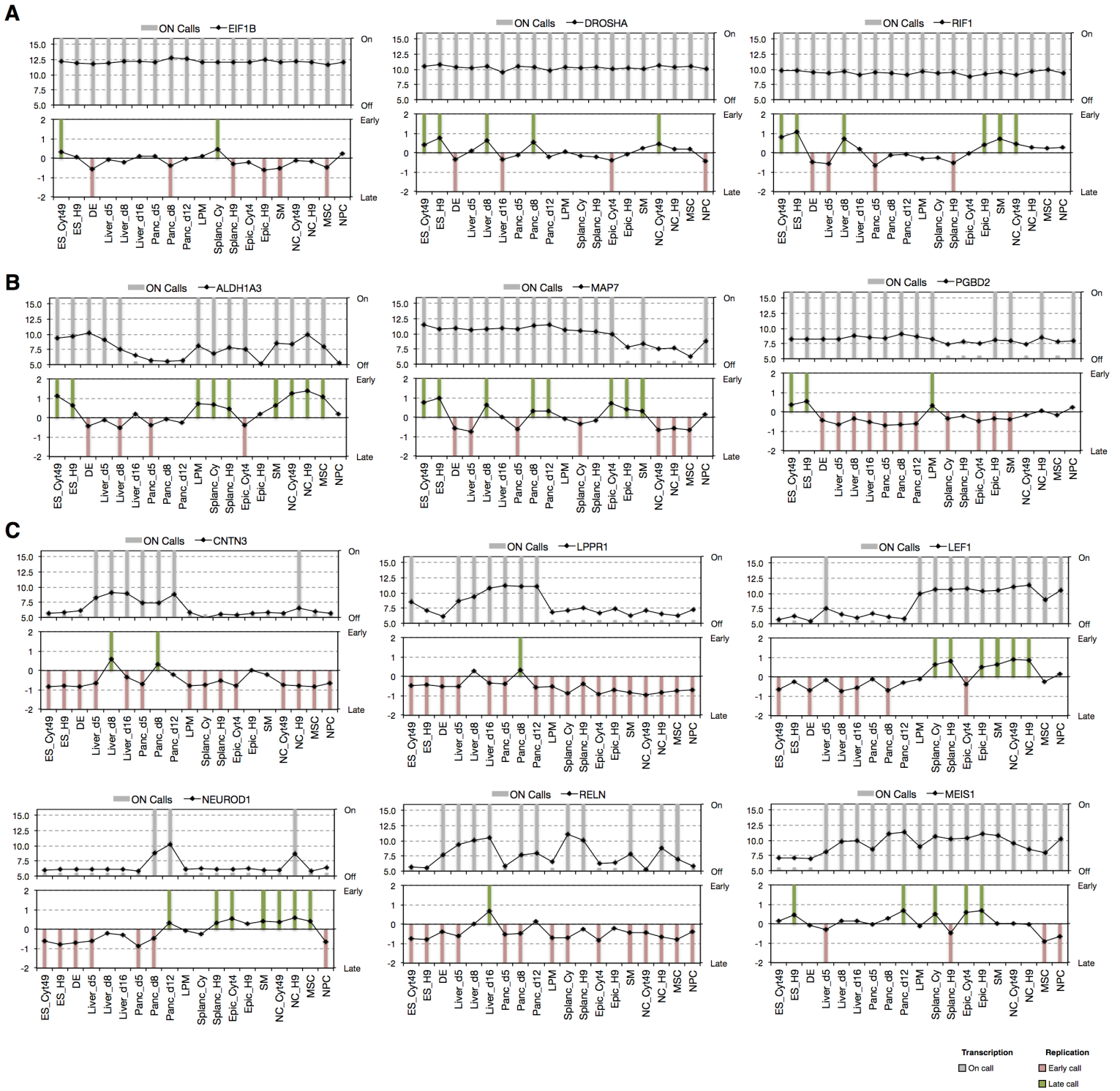
C



Supplementary Figure 16

Transcriptional and RT dynamic changes in endoderm (B), mesoderm (C) and ectoderm (D) per RT switching class. The genes with a fold difference ≥ 6 compared with hESC were classified into the RT clusters from Figure 4B-D and separated in the distinct categories of RT-switching genes to identify the kinetics of regulation.

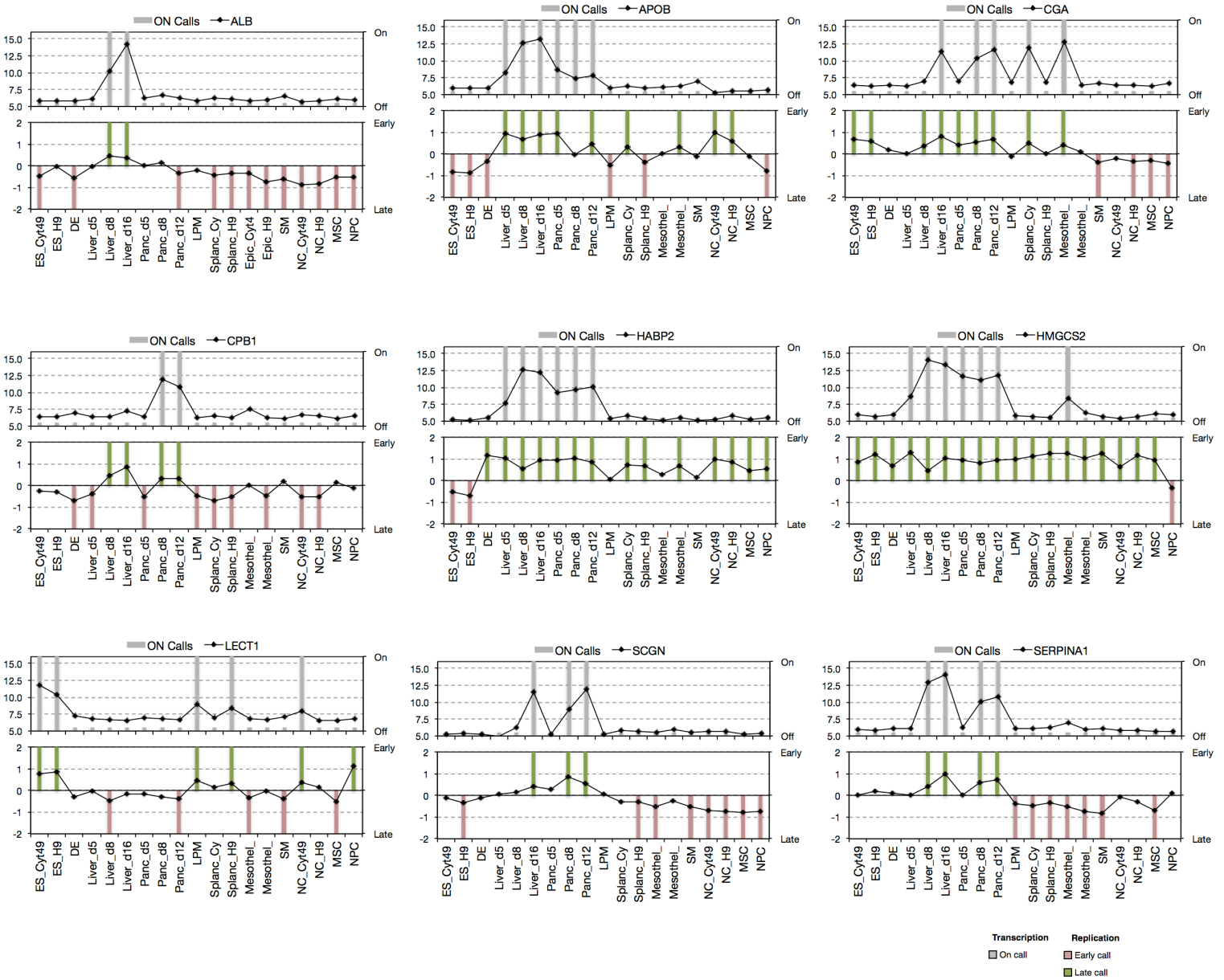
Supplementary figure 17



Supplementary Figure 17

RT and transcription regulation of C-class genes. A) Exemplary C-class genes that are not affected by RT changes. B) Exemplary C-class genes that retain expression after EtoL changes. C) Exemplary C-class genes that are induced before the LtoE RT changes.

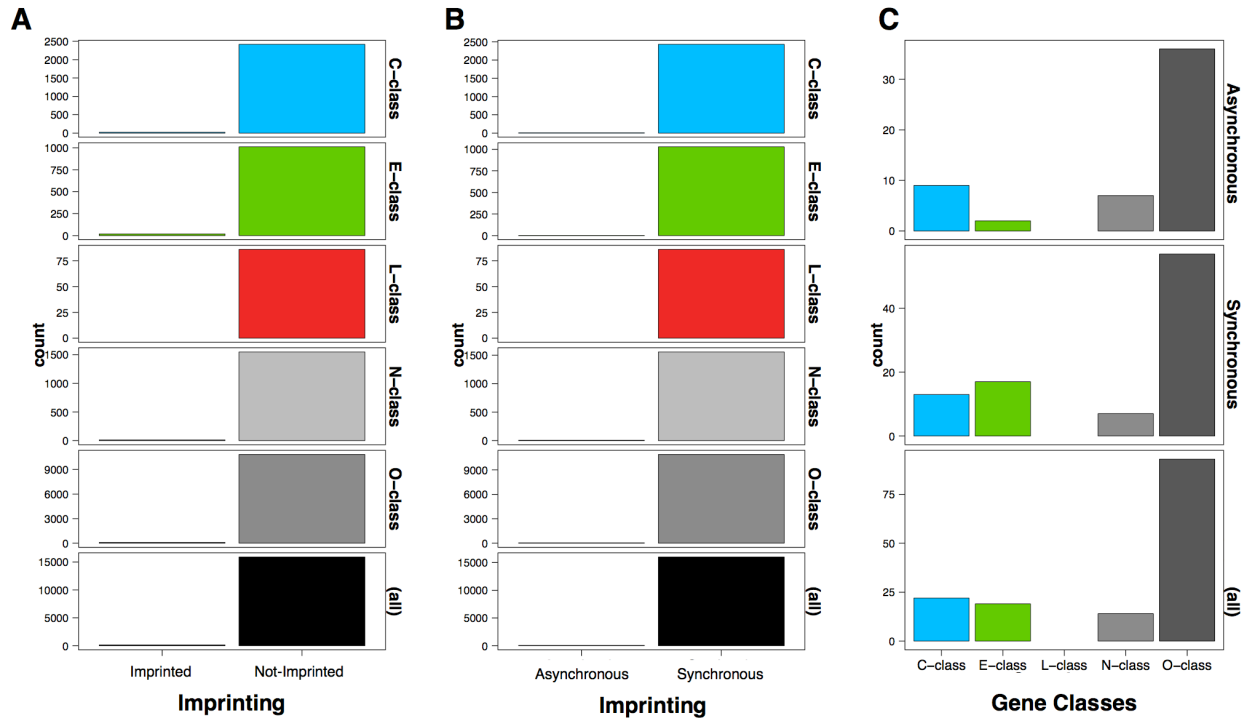
Supplementary figure 18



Supplementary Figure 18

RT and transcription regulation of E-class genes. Exemplary E-class genes that are highly expressed only when they switch to early replication.

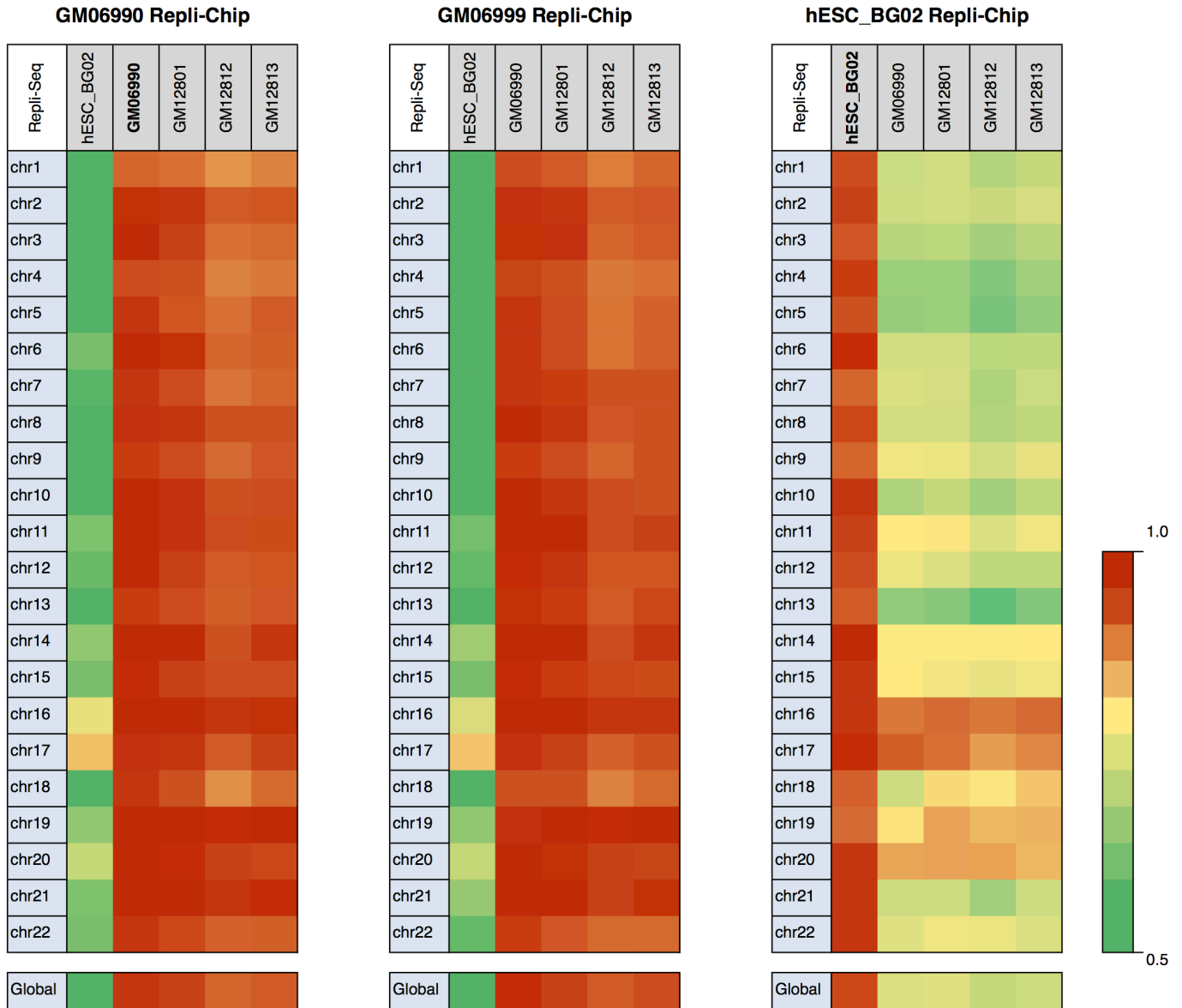
Supplementary figure 19



Supplementary Figure 19

Comparison of the distinct categories of genes (C, E, L, O-class) to imprinted genes. A) Distribution of imprinted vs. non-imprinted genes among the distinct classes of genes. B) Distribution of asynchronous vs. synchronously replicated genes among the distinct classes of genes. C) Distribution of imprinted genes into the distinct classes of genes. Imprinted and asynchronously replicated gene lists were extracted from Mukhopadhyay et al. 2014 and the imprinted genes database: <http://www.geneimprint.com>.

Supplementary figure 20



Supplementary Figure 20

Comparison of Repli-Chip and Repli-Seq datasets. Correlations per chromosome are shown for three distinct cell types, the Repli-Chip datasets are labeled on top and each column have the calculated values against distinct Repli-Seq datasets.